Enhancing photocurrent transient spectroscopy by electromagnetic modeling

H. Diesinger,[1,a)] M. Panahandeh-Fard,[2] Z. Wang,[2] D. Baillargeat,[1] and C. Soci[1,2,b)]
[1]*CINTRA CNRS/NTU/THALES, UMI 3288, Singapore*
[2]*Division of Physics and Applied Physics, Nanyang Technological University, Singapore*

(Received 17 January 2012; accepted 16 April 2012; published online 3 May 2012)

The shape and duration of photocurrent transients generated by a photoconductive switch depend on both the intrinsic response of the active material and the geometry of the transmission line structure. The present electromagnetic model decouples both shape forming contributions. In contrast to previously published work, it accounts for the particular operating mode of transient spectroscopy. The objective is to increase the time resolution by two approaches, by optimizing structural response and by deconvolving it from experimental data. The switch structure is represented by an effective transimpedance onto which the active material acts as current generator. As proof of concept, the response of a standard microstrip switch is modeled and deconvolved from experimental data acquired in GaAs, yielding a single exponential material response and hence supporting the validity of the approach. Beyond compensating for the response deterioration by the structure, switch architectures can be *a priori* optimized with respect to frequency response. As an example, it is shown that a microstrip gap that can be deposited on materials incompatible with standard lithography reduces pulse broadening by an order of magnitude if it is provided with transitions to coplanar access lines.
 [http://dx.doi.org/10.1063/1.4710996]

I. INTRODUCTION

Photoconductive switches are part of many THz generation setups involving laser pulses and can generate the large spectrum contained in a short photocurrent transient when excited by ultrashort laser pulses[1–3] or a coherent signal by difference frequency generation.[4,5] The generation of short transients and high frequencies depends on both a short carrier lifetime in the active region and a high bandwidth transmission line architecture. After the demonstration of the photoconductive switch by Auston,[6] efforts to increase the bandwidth have aimed at reducing the carrier lifetime in the active area by radiation damage,[7] amorphization,[8] and low temperature crystal growth.[9]

Photoconductive gaps are also deposited on semiconductors with unknown properties to determine their photoelectric responsivity. In the domain of organic semiconductors, photocurrent transients contain information about competing processes such as charge carrier generation shortly after photoexcitation, trapping, and recombination. The comprehension of these phenomena at the picosecond timescale is crucial for device performance of organic photodetectors and solar cells.[10–12] At present, the time resolution of photocurrent transient spectroscopy using plain microstrip lines has been reported to be of 100 ps.[12] In a switch architecture featuring coplanar access, 14 ps resolution has been reported.[15] The 14 ps response time coincides with the oscilloscope time resolution. Time domain terahertz spectroscopy on coplanar lines with optical sampling of the pulse has enabled response times of 1.5 ps (Ref. 14) and 500 fs.[13] However, the line spacing and gap sizes of these coplanar structures are too small to be obtained by shadow mask deposition. They require the use of lithography, disqualifying them for deposition on organic semiconductors due to the incompatibility with organic resist development and lift-off.

In the following, we develop a hybrid model that splits the behavior of the photoconductive switch into the responsivity of the active material and the transimpedance of the transmission line structure. We demonstrate the benefit in two ways. First, the simulated impulse response of a microstrip gap switch is deconvolved from an experimental transient of a GaAs switch, reducing the intrinsic photocurrent transient to a single exponential; this material response is in agreement with the expected behavior and shows the ability to improve temporal resolution. Second, a microstrip gap with dimensions compatible with shadow mask deposition on organic semiconductors is provided with a transition to coplanar terminals. As a consequence, its transimpedance bandwidth is predicted to increase by an order of magnitude, an effect which is supported by previous experimental observations.[13–15] Finally, the potential performance increase of photocurrent transient spectroscopy due to switch architectures optimized by electromagnetic modeling is discussed.

II. OBJECTIVES AND REQUIREMENTS

- The model must include the temporal response of the active material in the gap since this accounts for a part of the overall response and in some cases is the objective of the transient generation.
- The frequency response of a photoconductive switch with respect to the frequency of an applied input

a)Electronic mail: heinrich.diesinger@ntu.edu.sg.
b)Also at Division of Microelectronics, Nanyang Technological University, Singapore.

signal has been studied previously.[16] However, in transient spectroscopy the active material is used to generate a photocurrent transient, while the DC bias can be assumed to remain relatively constant. Consequently, the response with respect to an incoming ac signal is not required.

- Previous works have described the gap material as an S-matrix. This description introduces frequency response with respect to an applied ac signal. On the other hand, it implies linear bias dependence. Therefore, this description of the gap material is not suitable to study the carrier dynamics dependence on bias and will not be adopted.

Based on these requirements, the active region is described as a current generator. This allows taking into account nonlinear effects of the dc bias. The transmission line structure will be described as transimpedance derived from S-parameters.

III. HYBRID MODEL OF THE SWITCH

The decomposition of the photoconductive switch into active area and surrounding waveguide structure is shown in Fig. 1. The active area (indicated as oval spot) acts as a current generator, and the surrounding structure as a 4-port S-matrix. When a current is generated in the gap and applied to the edges of the waveguide, the structure transmits a wave propagating to the load on port 2. In the equivalent circuit in panel (b), the current generator across the gap is represented by two current generators applied in opposite direction to ports 3 and 4. The RF coupling across the gap determines the conversion of the photocurrent into a propagating wave towards the load. The aim of our work is to express the conversion between current and outgoing wave as a transimpedance spectrum. Previous works have approached the gap as a capacitor. However the geometry cannot be accounted for by a plane capacitor model and the lumped element approach cannot be expected to yield a good description of the entire electromagnetic coupling between the portions of waveguide facing each other. Therefore, we chose to rigorously compute the coupling by electromagnetic modeling using Ansys HFSS.[17] The description of the structure as a 4-port S-matrix allows to include a transmission line length sufficient for adequately describing the electromagnetic coupling, and simultaneously to apply the generated current to the very edges of the transmission line. As first estimate for the minimum length to be included into the computational volume, a length of twice the substrate thickness on each side of the gap is considered as the limit: at a wavelength much larger than the lateral dimensions of the waveguide, it can be considered that an open end emits an evanescent wave with a decay length of the order of the lateral confinement. The computational volume must include the portion of the opposite waveguide that is exposed to non-negligible evanescent field. An empirical approach of verifying the computational volume sufficiency is given in the discussion.

IV. TRANSIMPEDANCE AND IMPULSE RESPONSE OF THE STRUCTURE

The wave equilibrium on which the calculation of transimpedance will be based is shown in Fig. 2. The power wave formalism of scattering theory is employed.[18] Particular care has been taken in choosing the necessary waves to be taken into account for a *transient* analysis. The cables to bias source and oscilloscope are considered impedance matched to the microstrip line impedance Z_T and reflection at the bias source or oscilloscope is not taken into account. Therefore, we include only outgoing waves on ports 1 and 2. This approximation is justified, since the propagation delay over the transmission line length and the even longer one over the cable length (to bias source and oscilloscope) is much larger than the expected duration of the transient. Therefore, multiple reflection at the access ports 1 and 2 or even at the dc supply and oscilloscope can be safely neglected because their effect would be to generate ghost transients clearly discernible in time from the initial transient. Consequently, any reflection and hence insertion loss at these locations would merely effect the amplitude of the main transient but not its shape.

The current generators connected to ports 3 and 4 are described as infinite impedance with a resulting unity reflection coefficient. This description is exact: the coupling between the adjacent ports 3 and 4 is fully described by the S-Matrix itself and does not enter into the description of the current generator. Furthermore, we apply the principle of superposition: the current generation between microstrip edges on Fig. 1(a) is decomposed into two current generators on ports 3 and 4 in Fig. 1(b). In Fig. 2, only the current generator on

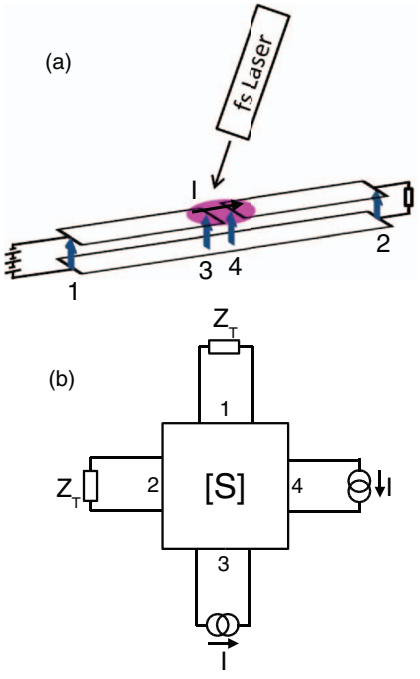

FIG. 1. Approach of modeling a photoconducive gap in a microstrip as 4-port S-matrix: (a) schematic of the microstrip gap with active material (oval spot) with port assignment; (b) equivalent circuit; outer ports 1 and 2 are considered to be terminated with the transmission line impedance Z_T, while inner ports 3 and 4, located at the transmission line edges, are open.

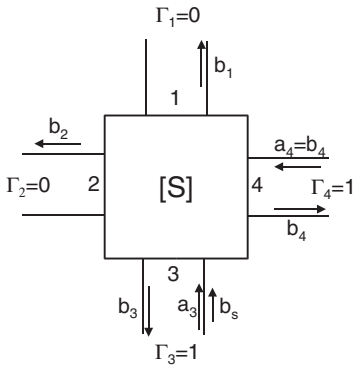

FIG. 2. Wave schematics depicting the equilibrium of incident and outgoing waves on the 4 port matrix. The current generation in the active medium is represented by the two opposed current generators on port 3 and 4.

port 3 is taken into account by the incident wave b_s that it generates. Later, the effect of an incident wave on port 4 is derived and finally both contributions are superposed. Taking into account these conditions, the transimpedance computation will be based on the following system of 5 linear equations for 6 power waves (b_1 is the wave towards the source and is not needed):

$$b_2 = S_{23}a_3 + S_{24}a_4, \tag{1}$$

$$a_4 = b_4, \tag{2}$$

$$b_4 = S_{43}a_3 + S_{44}a_4, \tag{3}$$

$$a_3 = b_s + b_3, \tag{4}$$

$$b_3 = S_{34}a_4 + S_{33}a_3. \tag{5}$$

First, the ratio between an outgoing wave on port 2 and the incident wave on port 3 is calculated by triangularizing the equation system

$$\frac{b_2}{b_s} = \frac{S_{23}(1 - S_{44}) + S_{24}S_{43}}{(1 - S_{44})(1 - S_{33}) - S_{34}S_{43}}. \tag{6}$$

Then the same reasoning will be repeated for the ratio between an outgoing wave on port 2 and a wave incident on port 4. The result can be obtained by swapping indices 3 and 4 in Eq. (6). Then, the equations describing b_2/b_s are added to take into account the superposed effect of incident waves on both port 3 and 4. Simplifications apply due to symmetry, e.g., $S_{33} = S_{44}$ and $S_{31} = S_{42}$ and due to reciprocity, $S_{ij} = S_{ji}$. The result can be obtained by swapping indices 3 and 4 in Eq. (6). Then, the equations describing b_2/b_s are summed up to take into account incident waves on both port 3 and 4. Simplifications apply due to symmetry, e.g., $S_{33} = S_{44}$ and $S_{31} = S_{42}$ and due to reciprocity, $S_{ij} = S_{ji}$.

The ideal current generator generates an incident power wave b_s on ports 3 and 4,

$$b_s = I\sqrt{Z_T}. \tag{7}$$

The voltage wave propagating on the transmission line Z_T towards the oscilloscope is

$$v = b_2\sqrt{Z_T}. \tag{8}$$

The resulting transimpedance or ratio between generated current and output voltage is then

$$v_2 = I Z_T \frac{S_{31} - S_{41}}{1 - S_{33} + S_{34}}. \tag{9}$$

The transimpedance can then be obtained from the frequency dependent S-parameters simulated by HFSS. In this work, a microstrip gap with 100 μm width, 20 μm gap length, 350 μm GaAs substrate thickness was modeled. A total microstrip length of 5 mm including the microstrip portions on either side of the gap has been included into the computational volume. The resulting transimpedance spectrum is near Z_T at low frequency and has a cutoff frequency of about 7 GHz.[19]

The transimpedance is Fourier transformed to obtain the impulse response of the switch structure which is plotted in Fig. 3(a). The resulting response can be approximated by a piecewise function consisting of a $\tau_0 = 78$ ps linear rise followed by an exponential decay with time constant $\tau_1 = 55$ ps.

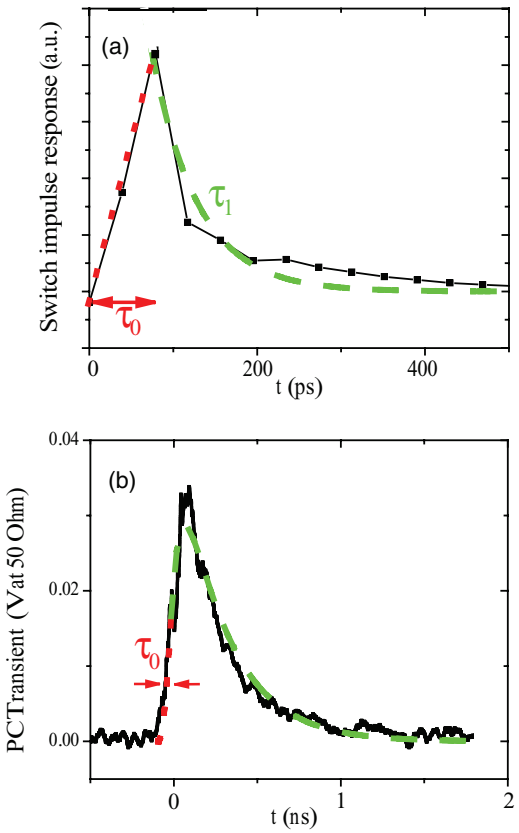

FIG. 3. Response functions: (a) modeled impulse response of the transmission line structure, and piecewise curve fit with a linear rise and an exponential decay; (b) measured PC transient of a Si-GaAs photoconductive switch, and curve fit with the piecewise defined structural response from the convolution product of the structural response of panel (a) and a single exponential decay with $\tau_2 = 279$ ps.

V. COMPARISON WITH EXPERIMENTAL DATA AND DECONVOLUTION

Experimental photocurrent transients have then been acquired in a photoconductive switch with the same dimensions as the one whose structural response has been computed. The microstrip structure was fabricated by evaporating 10 nm nickel and 1000 nm gold onto semi-insulating substrate. The gap was exposed to $\lambda = 800$ nm, $\tau_p < 100$ fs pulses at a 1 kHz repetition rate with 10 mW average power. The photocurrent transients have been acquired by a LeCroy WaveExpert 100H digital sampling oscilloscope and are plotted on Fig. 3(b). The measured photocurrent can be approximately described by a linear rise during 170 ps followed by an exponential decay with 298 ps time constant. In the following, the impulse response of the transmission line structure shall be deconvolved from the experimental transient to obtain the intrinsic response of the semi-insulating GaAs.

Since numerical deconvolution routines often require input functions with identical time intervals, symmetric response functions with an odd number of points and tend to diverge for noisy signals, we proceed the following way: the response function of the structure is analytically approximated by a combination of linear rise and exponential decay as shown in Fig. 3(a); the analytic function is convolved with a tentative material response function, in this case a single exponential decay with time constant τ_2. The resulting analytical description of the convolution product is then fitted to the experimental data to obtain the parameter τ_2 and to verify if the material response is adequately described by the proposed analytical function.

The piecewise definition of the switch response is a linear rise followed by an exponential decay

$$g(t) = \frac{A}{\tau_0} t \tag{10}$$

for $0 < t \leq \tau_0$, and

$$g(t) = A \exp - \frac{t - \tau_0}{\tau_1} \tag{11}$$

for $t > \tau_0$.

The intrinsic material response is expressed as a simple exponential decay function

$$f(t) = 0 \tag{12}$$

for $t < 0$ and

$$f(t) = \exp - \frac{t}{\tau_2} \tag{13}$$

for $t \geq 0$.

The functions are convolved stepwise and a time offset τ_{offs} is added since the time origin of the experimental transient signal is unknown *a priori*. The stepwise result for the convolution product then reads

$$h(t) = \frac{A\tau_2^2}{\tau_0} \left(\exp\left(- \frac{t - \tau_{\text{offs}}}{\tau_2} \right) - 1 + \frac{t - \tau_{\text{offs}}}{\tau_2} \right) \tag{14}$$

for $\tau_{\text{offs}} < t \leq \tau_0 + \tau_{\text{offs}}$ and

$$\begin{aligned} h(t) = {} & \frac{A\tau_2^2}{\tau_0} \left[\exp\left(\frac{\tau_{\text{offs}} - t}{\tau_2} \right) \left[1 + \exp\left(\frac{\tau_0}{\tau_2} \right) \left(\frac{\tau_0}{\tau_2} - 1 \right) \right] \right] \\ & + \frac{A}{\frac{1}{\tau_1} - \frac{1}{\tau_2}} \left[\exp\left(\frac{\tau_{\text{offs}} + \tau_0 - t}{\tau_2} \right) \right. \\ & \left. - \exp\left(\frac{\tau_{\text{offs}} + \tau_0 - t}{\tau_1} \right) \right] \end{aligned} \tag{15}$$

for $t > \tau_0 + \tau_{\text{offs}}$.

We note that the curve fitting is piecewise and that τ_{offs} is simultaneously a fitting parameter and a limit of the piecewise definition. Therefore, standard fitting routines cannot handle the fitting. Fitting has to be performed iteratively by piecewise fitting and alternately re-adjusting the fitting ranges, or very sophisticated tools would need to be used. Furthermore, during the fitting, the values of the fitting parameters τ_{offs} and τ_2 must be maintained identical for both fit ranges (τ_0 and τ_1 are fixed).

Figure 3(b) shows that a good agreement between the piecewisely defined convolution product and the experimental data are obtained for a material response well described by a single exponential decay function with time constant $\tau_2 = 279$ ps. This is consistent with a response function determined by intrinsic carrier lifetime of τ_2. Consequently, the benefit of the deconvolution is the determination of a single exponential with a decay time constant of $\tau_2 = 279$ ps compared to the 298 ps of the raw data which seems rather unspectacular as improvement. However, the finding of a single exponential signifies that the rise time of the material response is abrupt within the system resolution determined by the oscilloscope and the deconvolution procedure. The raw photocurrent has a rise time of about 170 ps. Equations (14) and (15) yield a rise time (from onset to maximum) of 161 ps of the convolved signal (fitted curve of Fig. 3(b)) with the determined parameters τ_0 to τ_2. We therefore confirm that the assumption of an abrupt rise of the material response is justified since the 9 ps misfit is within the accuracy of the method that cannot be better than the 15 ps time resolution of the 70 GHz oscilloscope plus the inaccuracies of the curve fit. Concluding that the material rise time is zero with an error of 9 ps describes the known material response of bulk crystalline GaAs, i.e., carrier generation at the sub-picosecond scale, >10 times more accurately than by attributing the entire experimental rise time of 170 ps to the material response. We cannot easily define an upper limit for the error of the rise time (e.g., set it equal to the oscilloscope resolution), since the treatment of error propagation throughout the fitting procedure, using partial derivatives with respect to each parameter, would be too tedious. We nevertheless emphasize that the deconvolution has the invaluable merit of preventing misinterpretations of the material response: for an unknown semiconductor with sub-picosecond carrier generation, all or the majority of the photocurrent rise time would be accounted for by the modeled structure response, and a remaining misfit of the order of the oscilloscope response would not be considered as proof of a mechanism of delayed or secondary carrier generation.

To test the sufficiency of the computational volume, transimpedance modeling was repeated while varying the computational volume. We have reduced the transmission line length included in the computational volume from 5 mm to 2 mm with almost no noticeable change in the amplitude of the transimpedance, suggesting that both lengths are sufficient to accurately describe the coupling of the transmission lines on either side of the gap.

VI. APPLICATION TO MATERIALS WITH NONLINEAR RESPONSE

The advantage that nonlinear effects can be taken in account does not affect the deconvolution procedure. We make the approximation that during the generation of a transient photocurrent at a given dc bias, this bias is large compared to the amplitude of the generated wave and hence the bias applied to the material remains rather constant. The validity of this assumption can be verified afterwards. Photocurrent transients can be generated and measured under different bias. The S-Matrix of the structure and hence the switch response is bias independent as per definition. A photocurrent transient of the active zone is obtained for each bias by deconvolving the constant switch response. By studying the bias dependence of the deconvolved photocurrent transient in the time domain, adequate models for nonlinear effects can be derived conveniently. This is a major advantage with respect to previous works reported in the literature: once the behavior of the medium is pounded into an inappropriate model such as an S-Matrix describing RF transfer from bias port to the oscilloscope that depends furthermore on light and dc bias, the recognition even of primitive effects such as carrier sweep out is considerably hampered.

VII. DESIGN OF NEW SWITCH ARCHITECTURES

The electromagnetic modeling framework developed so far can be applied to the design of novel switch architectures with higher performance. We have previously shown that switches featuring a transition to coplanar access improve the response.[19] The transmission line structure and the simulated structural impulse response of such a switch are shown in Fig. 4. The width of the impulse response of the switch with transition to coplanar access pads in Fig. 4(b) is about 15 ps, that is more than one order of magnitude smaller than the 300 ps response width of the switch with plain microstrip geometry in Fig. 3(a). Similar geometries are currently used for microwave switches, and the gain of an order of magnitude in response time predicted by our modeling is roughly in agreement with experimentally observed response times.[15] However, the modeled device has dimensions that allow defining the gap by multi-step metal deposition techniques: the coplanar access pads and transitions between coplanar and microstrip line can be pre-fabricated lithographically, whereas the actual gap is defined by a shadow mask on top of the drop cast organic semiconductor. The staircase shape of the transition is preliminary and has not undergone any optimization. Any further improvement of the response would immediately reduce the width of the response below the time resolution

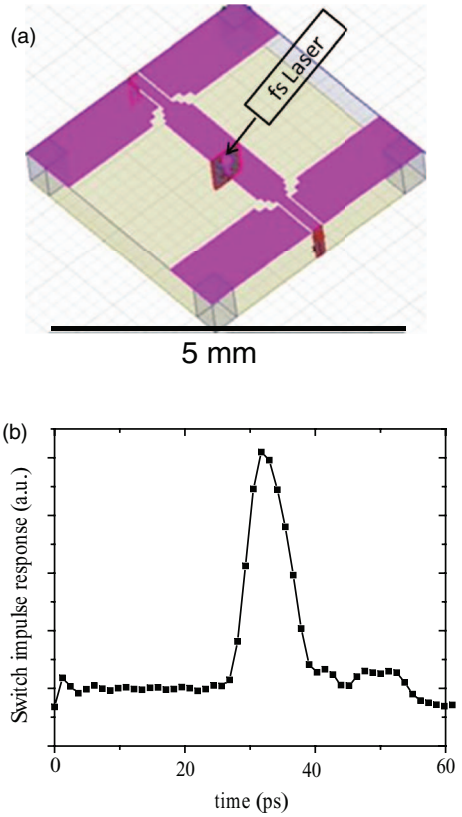

FIG. 4. Photoconductive gap in microstrip line featuring transitions to coplanar contact pads: (a) drawing of the modeled structure; (b) computed structural impulse response.

of oscilloscopes. Response times presently achieved exclusively by coplanar design are hence accessible by structures that can be fabricated by defining the actual gap on organic semiconductors by compatible deposition methods. Further optimization would make photocurrent transient spectroscopy on organic semiconductors eligible for being combined with optical pump-probe techniques.

VIII. CONCLUSION

The response of a photoconductive switch has been split into the intrinsic material response of the active area and a structural response, in a way adapted to the particular case where the switch is dc biased and used for generating transients under ultrashort laser illumination in order to determine the intrinsic material response. A hybrid model with the active area represented by a current generator, and the structure represented by a 4-port S-matrix, has been developed. The effect of the structure has been expressed as transimpedance. The expected impulse response of the structure has been deconvolved from an experimental photocurrent transient recorded in a GaAs switch, yielding a single exponential decay for the intrinsic material response. Although the reduction of the width of the photocurrent signal due to the deconvolution is unspectacular for the SI-GaAs switch used here, the photocurrent rise time has been reduced from 170 ps to an abrupt (resolution-limited) rise within the accuracy of the oscilloscope and the deconvolution procedure. This prevents falsely

attributing the switch structure response to the material, which can have disastrous consequences when studying mechanisms at the origin of photoconduction in unknown materials. The highest gain by the deconvolution procedure in terms of width reduction and accuracy can be expected for material responses of the same order of timescale as the structural response. Another use of modeling is the design of switches with better response. A switch whose gap can be defined on organic semiconductors by compatible deposition techniques, featuring coplanar access, shows a factor >10 improvement of response time over the plain microstrip structure. Further optimization has the potential of making photocurrent transient spectroscopy of organic materials compatible with the time resolution of optical pump-probe techniques and of bringing its time resolution to the same level as of indirect photoconductance measurements such as optical pump terahertz probe spectroscopy.

ACKNOWLEDGMENTS

The research was partially supported by the CNRS startup grant for CINTRA UMI 3288, the NTU NAP startup Grant No. (M4080511), and by the Funding of Initiatives in Support of NTU 2015 (M58110092). We thank Professor Wang Hong and Dai Xing for help in preparing the photoconductive switch. M.P.F. acknowledges financial support from a Yousef Jameel scholarship.

[1]J. A. Valdmanis, G. A. Mourou, and C. W. Gabel, IEEE J. Quantum Electron. **19**, 664 (1983).
[2]J. S. Melinger, N. Laman, S. S. Harsha, and D. Grischkowsky, Appl. Phys. Lett. **89**, 251110 (2006).
[3]J. F. Lampin, L. Desplanque, and F. Mollot, Appl. Phys. Lett. **78**, 4103 (2001).
[4]A. S. Weling and D. H. Auston, J. Opt. Soc. Am. **13**, 2783 (1996).
[5]E. R. Brown, A. McIntosh, B. Nichols, and C. L. Dennis, Appl. Phys. Lett. **66**, 285 (1995).
[6]D. H. Auston, Appl. Phys. Lett. **26**, 101 (1975).
[7]P. R. Smith, D. H. Auston, A. M. Johnson, and W. M. Augustyniak, Appl. Phys. Lett. **38**, 47 (1981).
[8]D. H. Auston, P. Lavallard, N. Sol, and D. Kaplan, Appl. Phys. Lett. **36**, 66 (1980).
[9]F. W. Smith, H. Q. Le, V. Diadiuk, M. A. Hollis, A. R. Calawa, S. Gupta, M. Frankel, D. R. Dyakaar, G. Mourou, and T. Y. Hsiang, Appl. Phys. Lett. **54**, 890 (1989).
[10]M. B. Sinclair, D. Mcbranch, T. W. Hagler, and A. J. Heeger, Synth. Met. **50**, 593 (1992).
[11]O. Ostroverkhova, S. Shcherbyna, D. G. Cooke, R. F. Egerton, F. A. Hegmann, R. R. Tykwinski, S. R. Parkin, and J. E. Anthony, J. Appl. Phys. **98**, 033701 (2005).
[12]C. Soci, I. Hwang, D. Moses, Z. Zhu, D. Waller, R. Gaudiana, C. J. Brabec, and A. J. Heeger, Adv. Funct. Mater. **17**, 632 (2007).
[13]G. A. Mourou and K. E. Meyer, J. Appl. Phys. **45**, 492 (1984).
[14]F. A. Hegmann, D. Jacobsperkins, C. C. Wang, S. H. Moffat, R. A. Hughes, J. S. Preston, M. Currie, P. M. Fauchet, T. Y. Hsiang, and R. Sobolewski, Appl. Phys. Lett. **67**, 285 (1995).
[15]V. J. Logeeswaran, A. Sarkar, M. S. Islam, N. P. Kobayashi, J. Straznicky, X. Li, H. Wu, S. Wei, S. Mathai, M. R. T. Tan, S. Y. Wang, and R. Williams, Appl. Phys. A **91**, 1 (2008).
[16]J. F. Roux, J. M. Delord, and J. L. Coutaz, IEEE J. Quantum Electron. **47**, 223 (2011).
[17]See http://www.ansys.com for product description and sales contact.
[18]W. S. C. Chang, *Fundamentals of Guided-Wave Optoelectronic Devices* (Cambridge University Press, 2010).
[19]H. Diesinger, M. Panahandeh-Fard, D. Baillargeat, and C. Soci, in *Proceedings of the 2011 IEEE MWP, Microwave Photonics, 18–21 October 2011, Singapore* (IEEE, New York, 2011), p. 373.